DEEJ (2022) 11 (7) 1-12

University of Kashan

Desert Ecosystem Engineering Journal

Journal homepage: http://deej.kashanu.ac.ir

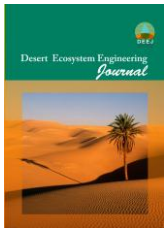

Investigating the Status of Desertification Vulnerability in JoghatayCounty, Iran

Mostafa Dastorani[1]

Received: 23/09/2021 Accepted: 26/12/2021

Abstract

This study sought to investigate the vulnerability of the Joghatay County, Khorasan Razavi, Iran, to desertification using several remote sensing products. To this end, sixMODISpotential indicators, including enhanced vegetation index (EVI), Vegetation Condition Index (VCI), salinity index (SI), Synthetized Drought Index (SDI), Temperature Condition Index (TCI), and precipitation rate of March 2020,were applied. These layers were then normalized and weighted using the Min-Max approach and Analytical Hierarchy Method, respectively. Finally, the vulnerability map was prepared via the weighted average method. The study's results indicated that the majority of the study area (67.5%) fell within the low to moderate vulnerability classes. However, the high-risk class area should be taken into account seriously, as it covers 365 km^2 (~21%) (one-fifth) of the whole study area.Moreover, the mountain foothills in the south and north of the area were classified within the high desertification vulnerability class, possessing the lowest vegetation density and highest temperature values. Nonetheless, the central areas with the greatest vegetation density formed the lowest desertification vulnerability as expected. The comparison of the ground truth values (some 200 points of the study area were randomly visited, and each of them was assigned a 0 or1 score)and the rated scores revealed more than 75% compatibility.Therefore, it could be argued that lack of vegetation due to climatic and edaphic measures and anthropogenic factors are responsible for the Joghatay region's high vulnerability to desertification.

Keywords: Geography, Degradation, Vegetation, Remote Sensing, Iran.

1. Assistant Professor, department of remotsensing, geographical and enviromental college, hakim sabzevari university. sabzevar, iran; m.dastorani@hsu.ac.ir
DOI: 10.22052/jdee.2021.243122.1077

1. Introduction

The issue of desertification was first brought to global attentionin1992 at the Global Earth Summit in Rio de Janeiro, where desertification and climate change were introduced as the greatest challenges facing the 21st century(ten Have et al., 2021). Theadoption of the United Nations Convention on Combating Desertification (UNCCD) was one of the major outcomes of the summit,which sought to evaluate and mitigate desertification worldwide, addressing specifically the arid, semi-arid, and dry sub-humid areas, known as the drylands, where some of the most vulnerable ecosystems and peoples can be found (Tollefson et al., 2012). According to UNCCD, desertification is defined as the degradation of land in arid, semi-arid, and dry-subhumid areas due to human interventions,including over-cultivation of land, overgrazing, and deforestation, among others (Vogt et al., 2011).

Caused by numerous natural and anthropogenic interrelated factors, desertification has several environmental, economic, and social consequences (Darkoh, 1998).Therefore, its careful analysis is of great importancefor both scientific and policy-making bodies. Different authorities have adopted various and mostly contradictory approaches to evaluate and map desertification, among which field study is believed to be the best and most accurate evaluation method. However, as it comes with tedious and cumbersome procedures,field study is not welcomed by researchers and land managers. Therefore, several modeling tools have been proposed to map land degradation and desertification at different scales quickly.In this regard, some attempts have been made at the international level to evaluate desertification, including the Global Assessment of Human-induced Soil Degradation (GLASOD) (Oldeman et al., 1991) and the Mediterranean desertification and land use (MEDALUS) approach (Kosmas et al., 1999). The same efforts have also been made in In Iran, includingthe Iranian Model of Desertification Potential Assessment (IMDPA), Iranian Classification of Desertification (ICD and its modified version MICD), and Iranian Research Institute of Forest and Rangelands Ekhtessasi – Ahmadi (IRIFR-EA) model (Fathi et al., 2015).

However, while the models have been proven reliable, they require a considerable amount of input variables, most of which are not readilyavailable in remote areas in arid lands. Therefore, there has been a growing interest in enjoying the benefits of advanced technologies in the field of mathematical, remote sensing, and geographic information system (GIS) sciences.

The advent of computers hasrevolutionized environmental studies beyond imagination. In fact, computers are quick and flexible in terms of data curation and handling, producing visual outputs that could not easily be obtained through the previous manual procedures (Gajos et al., 2012). On the other hand, the application of satellite data products in computer-based GIS systems and mathematical models has made it possible to evaluate different environmental issues in remote arid areas. Among the potential mathematical procedures mostcommonly integrated into the RS and GIS systems is the multi-criteria decision making (MCDM), in which multiple, often conflicting, alternatives in decision making are evaluated against each other in terms of several defined criteria and indicators. MCDMmethods are

advantageous in terms of their inherent simplicity and transparency and their fair and open process for evaluating options (Velasquez et al., 2013). The application of an MCDM method prepares the ground for the combination of several factors to find out the final vulnerability of the intended area to desertification and land degradation.

There has been a growing number of studies using remote sensing, GIS, and MCDM methods in evaluating desertification vulnerability, including Akbari et al. (2021), Akbari et al. (2020), Chen et al. (2019), and Shihab et al. (2020). However, while there are a considerable number of studies regarding desertification assessment, remote sensing products have rarely been used in studies conducted on the desertification evaluation in arid lands, especially in Iran. Therefore, the current study sought to evaluate the applicability of remote sensing products in an arid area to prove the products' potentials for robust and prompt mapping of desertification.

The study area of this research is located in some Iranian arid areas with desertification records.The area was selected because it has been experiencing a growing trend of land degradation, indicated by growing soil salinity, water and wind erosion, and a lowering rate of land fertilization (Kaviani et al., 2014). However, the area's remoteness has made it extremely difficult to collect data via field reconnaissance, and, therefore, remote sensing methods were of utmost importance for assessing the area's desertification. The results of this study will help land managers quickly evaluate desertification in the area, determine different factors'trends, and map desertification with unprecedented accuracy. Moreover, this method could easily detect any expansion of or retreat in desertification.

2. Materials and Methods

2.1. The Study Area

The study area is the Joghatay County of the Khorasan Razavi Province, located between 36º 25" and 36º 55" N and 56º 50" to 57º 20" E with a total area of 1715 km^2 (Figure 1). The area's precipitation rate ranges from 164 mm in the north to 483 mmin the south. The area is bounded from the north and the south by minor elevations and the Kalshur River in Sabzevar, respectively. The Joghatay's heights are parallel to the Al-Adagh-Binalood mountain range extended from northwest to the southeast direction, with its width varying from 12 km to 30 km, separating the Sabzevar plain from the Jovin plain. Moreover, the region reaches Esfarayen city, Sabzevar plain, Khoshab city, and Miami county in Shahroud city from the north, south, east, and the west, respectively. The highest altitude point of the region is called Koohgar, with a height of 2480 meters, and its lowest altitude is located in the south of the same region in the Mazinan desert, possessing an 800-meter height in an area measuring 1324 square meters.

Geologically, the study area is considered a rugged area in Central Iran, scattered in triangular forms inside the Iranian plateau. Fractures, faults, and folds are regarded as some features of this geological unit, which are characterized by tectonic fractures in rocks. Moreover, the area's vegetation exists in the form of very sparse patches dominated by *Artemisia Sidberi*, *Elaeagnusangustifalia*, *Astragalus* spp., and*Pegaumgoeblia* species.

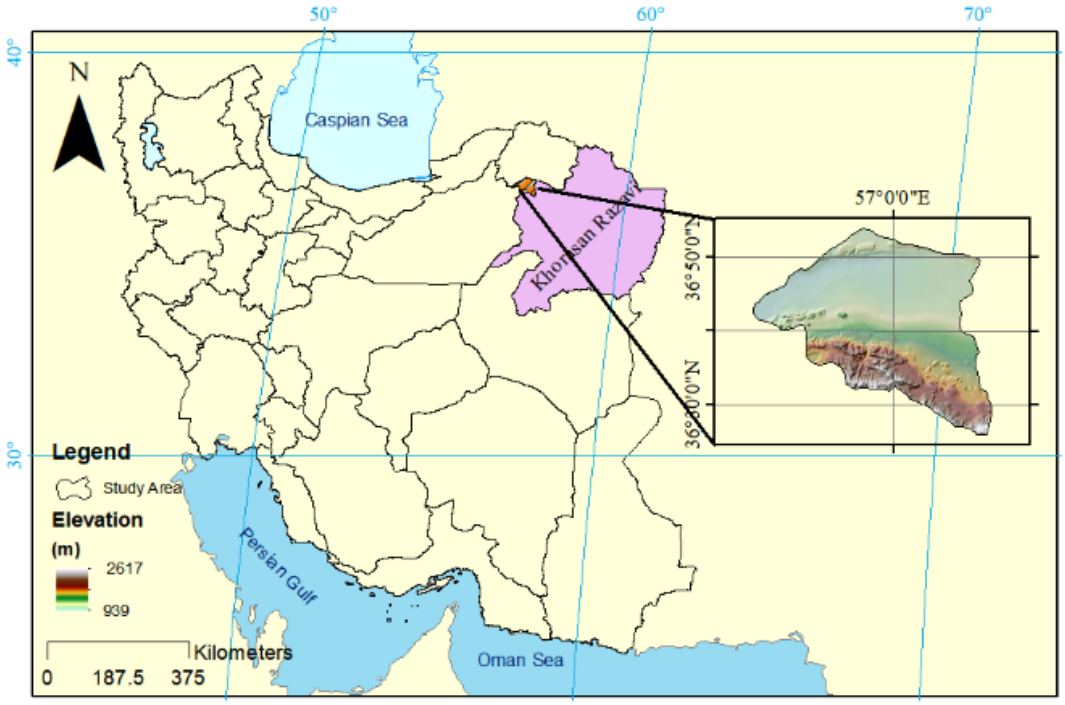

Figure (1): Location of Joghatayarea in Khorasan Razavi Province,Iran, and the area's elevation map

2.2. Data Collection

This study used six potential indicators, including theEnhanced Vegetation Index (EVI), Vegetation Condition Index (VCI), Salinity Index (SI), Synthetized Drought Index (SDI), Temperature Condition Index (TCI), and precipitation. Moreover, MODIS satellite EVI product (MOD13Q1), Modis NDVI product (MOD13A3v006), MODIS Land Surface Temperature (LCT) product (MOD11A2), and Modis MOD13Q1 product were used to calculate the salinity index from https://modis.gsfc.nasa.gov. The required data was collected fromMarchwhen the vegetation usually grows fully. Precipitation data were also collected from eighty-threeclimatic stations inside and around the area (data obtained from Iran's Meteorological Organization). In addition, thedata produced by Shuttle Radar Topography Mission (SRTM) 1 Arc-Second was obtained from https://srtm.csi.cgiar.org/. All the processes were performed in ENVI 5.3 and ArcGIS 10.3 software.

2.3. Method

2.3.1. The applied indicators

2.3.1.1. Enhanced Vegetation Index (EVI)

As it is not sensitive to vegetation changes, atmospheric conditions, and noise, EVI is preferable to the conventional Normalized Vegetation Index (NDVI). The index is calculated as follows:

$$EVI = G\frac{NIR-Red}{NIR+C_1Red-C_2Blue+L} \quad \text{(eq. 1)}$$

where NIR, Red, and Blue are the full or partially atmospheric-corrected surface reflectance, L stands for the canopy background adjustment for correction of the nonlineardifferential NIR, differential NIR and red radiant are transferredthrough a canopy, C_1 and C_2 are the coefficients of the aerosol resistance terms, and G is the gain or scaling factor. The coefficients adopted in calculating EVI products are L=1, C_1=6, C_2=7.5, and G=2.5. (Didan et al., 2015). The index ranges from zero to one, with

vegetation with higher densities obtaining higher values. The Modis product for the year 2020 was also obtained. However, as the product's data of the year was only available every 16 days, the weighted average method was used to convert the data into its monthly equivalent.

2.3.1.2. Vegetation Condition Index (VCI)

The main purpose of this index is to evaluate the vegetation growth in response to climatic changes and the vegetation evolution in response to the maximum and minimum growth potential defined by ecological constraints (Kogan, 1995). the index is calculated as follows:

$$VCI_i = \frac{NDVI_i - NDVI_{min}}{NDVI_{max} - NDVI_{min}} \quad \text{(eq. 2)}$$

where VCI_i stands for vegetation conditionin the ith year of the study period, $NDVI_i$ is the NDVI's value for each pixel in the ith year, and$NDVI_{max}$ and $NDVI_{min}$ are the maximum and minimum NDVI values throughout the study period, respectively. The monthly VCI product was used for calculating the index.

2.3.1.3. Precipitation

The correlation between altitude and precipitation was measured among 83meteorological stations inside and around the area (Khorasan Razavi Province) to prepare theregion's interpolated precipitation map. Figure 2 shows the correlation between altitude and precipitation within the meteorological stations. The error rate (R^2) of 0.71 indicatesan acceptable accuracy level.

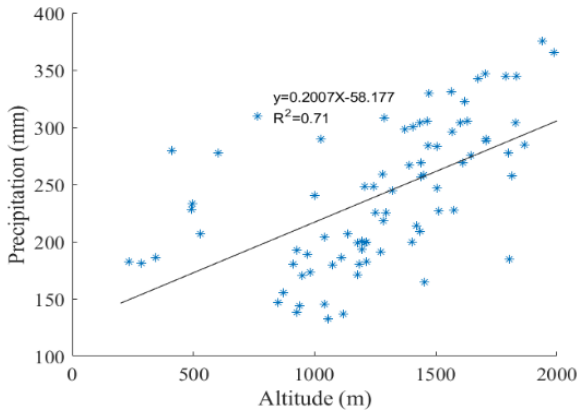

Figure 2. Correlation between altitude and precipitation inKhorasan Razavi's83 meteorological stations

2.3.1.4. Temperature Condition Index (TCI)

The Temperature Condition Index (TCI) (Kogan, 1995) is complementary to the VCI inevaluating drought severity. Here, areas with a higher desertification risk lose their soil moisture and display thermal tension at the ground level, increasing air temperature. The MODIS Land Surface Product was used at 1 Km resolution by eightdays intervals to calculate the index. The data were then converted to their monthly equivalent. TCI is calculated as follows:

$$TCI_i = \frac{LST_{max} - LST_i}{LST_{max} - LST_{min}} \quad \text{(eq. 3)}$$

where TCI_istands for the temperature conditionvalues in the i^{th} year, LST_{max} is the maximum ground surface temperature value for each pixel throughout the study period, LST_i is the ground surface temperature value for each pixel in the ith year, and LST_{min} is the minimum ground surface temperature value for each pixel during the study period. Unlike NDVI, for TCI, the maximum and minimum surface temperature values occur during dry and normal years, respectively. The index ranges from zero to one, where drought conditions are roughly zero values, and the wet years are assigned values close to one.

2.3.1.5. Synthetized Drought Index (SDI)

The synthesized drought index (SDI) was obtained using the principal component analysis (PCA) test to remove the iterative information from all other indices. The PCA test was applied to NDVI and VCI as the vegetation assessment component, the LST data were used as the component of land-surface temperature analysis (TCI index), and the precipitation data were used as the precipitation assessment component (Precipitation). The results were found to be significant for VCI, TCI, and P (consistent with the findings of the study carried out by Du et al. (2013)).

2.3.1.6. Salinity Index (SI)

Salinization is the primary cause of desertification. An increase in soil salinity could be attributed to the parent materials, chemicals, improper irrigation, water quality, saline groundwater rise, etc. (Daliakopoulos et al., 2016; Wang et al., 2009). Therefore, the MODIS visible band product, which comes at 16-day intervals,was used to calculate the area's salinity index (SI). The collected data were then converted to their monthly equivalent using the weighted average method. Moreover, the product's500-meter-resolution bands (red band 4 and blue band 6) were used. SI is calculated as follows (Mehta et al., 2013):

$$SI = \sqrt{BLUE * RED} \qquad \text{(eq. 4)}$$

where RED and BLUE are the red and blue bands of MODIS images.

2.4. Normalization

For the RS thematic layers to be combined, the layers must have a common measurement scale.The process of converting the collected data into a comparable range of values is called standardization. There are several standardization procedures such as Min-Max, Z-score, Median Normalization, Fuzzy Transform, etc. (Jain et al., 2005), from among which the Min-Max method was used in this study to standardize the layers, which is the simplest yet the most consistent standardization method in rescaling the range of values into a scale of 0 to 1, and defined as:

$$x' = \frac{x - \min(x)}{\max(x) - \min(x)} \qquad \text{(eq. 5)}$$

where x stands for the original value, and x' is the normalized value.

2.5. Scaling

Combining standardized layers requiresthe identification of each indicator's significance in the final decision. The Analytic Hierarchical Process (AHP) and the Analytic Network Process (ANP) developed by Saaty (Saaty, 2008) are the most widely-used methods in this regard. Since the results of the ANP method is more complicated to interpret than that of the AHP (Görener, 2012), the weight of different indicators was measured using the AHP method. Then, according to Table1, each indicator was assigned a score from 1 to 9 by five experts familiar with the topic and the study area. The results were analyzed using the Expert Choice 11.0 software. The comparisons are considered to be valid as long as the inconsistency between judgments remain low, which was evaluated via Consistency Ratio (CR).

Table (1): The scoring scheme used for generating pairwise comparison matrices in the AHP approach (Jafari Shalamzari et al., 2019)

Scores	*Importance*
1	Equally important
3	Moderately more important
5	Strongly More Important
7	Very strongly more important
9	Extremely more important
2,4,6,8	Intermediate values between two levels of importance

2.6. Combination

The final desertification intensity was calculated using the weighted overlay combination as follows (eq. 5):

$$DI = \sum_{i=1}^{n} W_i \times y_i \qquad \text{(eq. 5)}$$

where W_i is the weight assigned to each layer, and $y_i$stands for the standardized layer.

3. Results

3.1. Weights

Table 2 shows the results of the AHP method.Accordingly, vegetation indices (including the VCI, EVI, and SDI) and precipitation received the highest weights (0.25, 0.18, and 0.25), while salinity indexand TCI received the lowest values. Therefore, according to the experts, lack of vegetation and precipitation are the main driving forces of desertification in the area. Given that the CR was reported to be 0.06, the judgments are considered valid.

Table (2): The reported weights of the thematic layersobtained from the AHP method tomeasure desertification intensity in Joghatay, Iran

Indices	*TCI*	*VCI*	*EVI*	*SDI*	*P*	*SI*	*Total*
Weights	0.0977	0.2582	0.1846	0.1346	0.2559	0.0644	1

CR=0.06

3.2. Distribution of area among different classes

The indicators were divided into several classes according to the literature review, the results of which are presented in Table 3. Accordingly, most of the area was classified as low to moderate drought in terms of TCI, SDI, and VCI, indicatinga minor limitation in this regard. As for the EVI, more than 81% (1398 km2) of the area had low to moderate vegetation density. The salinity index also suggested no limitation in the area, as the whole area fell into the low to moderate class.

Table (3): Distribution of land area in different classes of desertification assessment indicators in 2020 in Joghatay, Iran

Class	*R*	*TCI*	*SDI*	*VCI*	*Class*	*R*	*EVI*	*Class*	*R*	*Salinity*
Extreme D.	0-0.1	0	9.7	29.3	Very Low	0-0.2	309.8	Low	0-0.17	1667.4
Severe D.	0.1-0.2	0	1.6	265.3	Low	0.2-0.4	1286.7	Moderate	0.17-0.2	47.3
Moderate D.	0.2-0.3	0.1	64.5	1157.5	Moderate	0.4-0.6	111.4	High	0.2<	0.1
Mild D.	0.3-0.4	11.5	631.1	241.4	High	0.6-1	6.9			
Abnormal D.	0.4-0.5	328.0	1007.6	21.3						
NoD.	0.5-1	1375.1	9.7	29.3						

R = range D=Drought;Enhanced vegetation index (EVI), Vegetation Condition Index (VCI), salinity index (SI), Synthetized Drought Index (SDI), Temperature Condition Index (TCI), precipitation (P)

Figure 3 shows the results of the normalization process.As shown for the TCI index (Figure 3 A and Table 3), most of the area falls within the No Drought index class. The same results were obtained for the synthesized drought index (calculated by combining VCI, TCI, and P). The salinity index's map also shows that salinity is the least important index in the study area due to the fact that its normalized range is only up to 0.22. However, since most of the area is covered with very sparse vegetation, the VCI index received low values in most of the area except for some small areas in the central plain. The same is also applicable to the EVI, where only some small areas in the central plain received high values. As for the precipitation index, it was found that all parts suffered from precipitation scarcity except the southern elevations of the study area

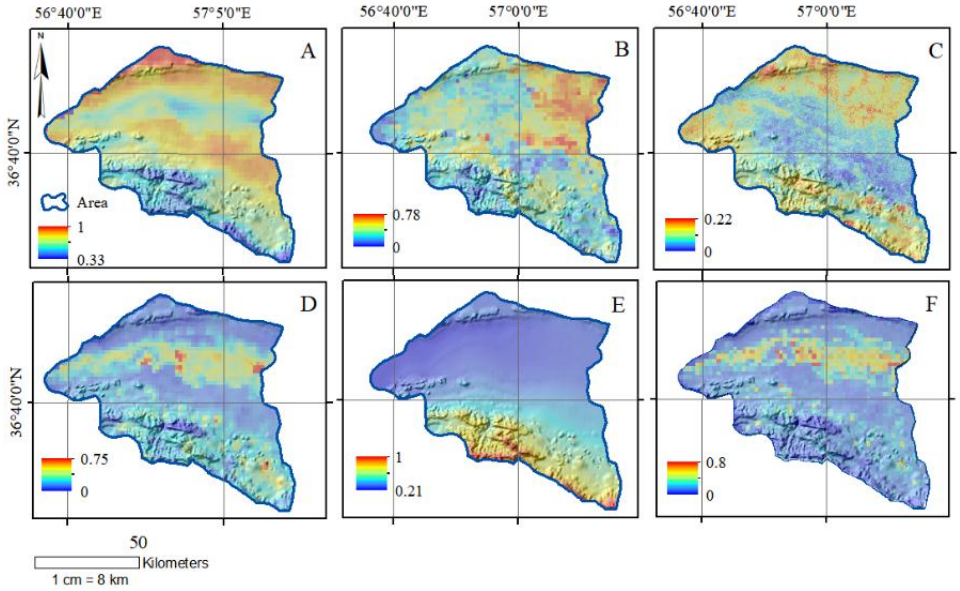

Figure (3): Standardized thematic layers used to evaluate desertification in Joghatay, Iran TCI(A), SDI (B), Salinity (C), VCI(D), Precipitation (E), EVI (F)

3.3. Desertification Map

Figure 4 shows the results of the thematic layers' weighted overlay combination used to evaluate desertification in Joghatay, Iran. The map was classified into four categories, ranging from no desertification vulnerability to highvulnerability. As shown in Figure 4, the majority of the area (67.5%) fell under the low to moderate vulnerability classes. However, the area classified as high-vulnerability should be taken into account seriously since 365 km^2(~21%) of the area covers more than one-fifth of the whole area. As presented in Figure 4, the mountain foothills fall within the high desertification vulnerability class in the south and north of the area with the lowest vegetation density and highest temperature values, while, as expected, the central areas were classified within thelowest desertification vulnerability class, with their vegetation density found to be at the greatest level.

Table (4): Distribution of the area among different desertification classes in the Joghatay region

Class	*No. of Pixels*	*Area*	*Relative Percentage*
No-Risk	4599	243.3	14.2
Low Risk	11001	581.9	33.9
Moderate Risk	9914	524.4	30.6
High Risk	6903	365.1	21.3
Total	32417	1715	100

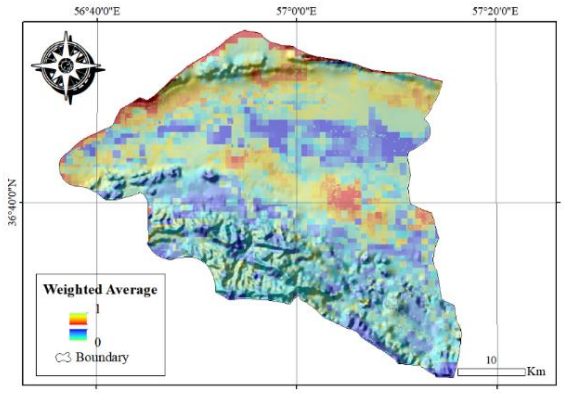

Figure (4): Final desertification map prepared by combining the included thematic layers in Joghatay, Iran

4. Discussion

Based on the combination of six products of TCI, VCI, EVI, SDI, Precipitation, and SI, the Joghataycounty was evaluated in terms of vulnerability to desertification. Accordingly, the greatest importance was given to the precipitation, VCI, and EVI. Precipitation is a primary source of concern in the area since most of the area had low suitability values,experiencing merely 164 mm rainfall every year. Thus, lack of precipitation is the main reason behind low vegetation in the region, facilitating other driving forces of desertification (Parvari et al., 2011)

VCI is used to compare the vegetation condition of a given year with its previous values throughout the same period in terms of maximum and minimum vegetation (Orimoloye et al., 2021). Therefore, VCI values for the year 2020 indicate a range from minimum to maximum possible vegetation in the area. Accordingly, low VCI values suggest severe drought and vulnerability to desertification. Therefore, as most of the area falls within the moderate to severe drought classes, it could be concluded that Joghatay is vulnerable to desertification.

As land surface temperatures may result in considerable soil moisture loss because of evapotranspiration, TCI could be a proxy for soil moisture tension (Ferreira et al., 2017). Considering the fact that most of the area falls within the low TCI class, soil moisture loss is not a significant issue due to its significantly low precipitation level. Moreover, SDI, which is obtained through the combination of the VCI, TCI, and precipitation (similar to Du et al. (2013)),did not indicate vulnerability to desertification since the normal classes occupied almost 85% of the area.

As a complement to NDVI, EVI accounts for chlorophyll concentrationandleaf area, and removes background noise (Abdollahi et al., 2019a, 2019b). Since it is more sensitive to high and low biomass levels, EVI could be a suitable alternative for NDVI in arid areas. Accordingly, the results of EVI analysis suggested that lack of vegetation was a significant limitation in the region, as more than 78% of the area fell within the very low and low vegetation classes. Furthermore, no considerable limitations were found in the area in terms of salinity.

The regional desertification vulnerability map was prepared by combining thematic layers, and the final vulnerability map was classified into four sub-classes. It was found that more than 50% of the area fell under the moderate to high vulnerability classes, which were mainly distributed on the foothills of the southern and northern elevations of the area. It seems that areas with lower EVI, VCI, and TCI values are responsible for their high vulnerability to desertification. The same results were obtained by Sepehr et al. (2012) and Sepehr et al. (2014). Moreover, Shiravi et al. (2017) found high desertification vulnerability in Khorasan Razavi Province by applying the same methodology. Similar tothe

current study's findings, Pashaei et al. (2017) found that more than 60% of Mashhad city (geographically close to the site) is vulnerable to desertification, applying the EVI, salinity, and LST during 2000-2013 period.

In order to validate the present study's findings, some 200 points of the study area were randomly visited, each of which was assigned a score from 0 and 1. Accordingly, more than 75% compatibilitywas found between the study'sfindings and the rated scores (according to the Kappa measure; see Dharumarajan et al. (2018), proving that the results of the study are reliable.

5. Conclusion

In this study, Joghatay'svulnerability to desertification was evaluated via several remote sensing products, using six MODISpotential indicators, including EVI, VCI, SI, SDI, TCI, and Pfor March 2020. The collected data were combined using the weighted overlay method, and the resulting map was classified into four severity classes ranging from low to high-risk desertification. Accordingly, the majority of the area (67.5%) was found to be under the low to moderate vulnerability classes. Whilethe high vulnerability class covers only ~21% of the total area, the area should be seriously taken into account, as 365 $km^2$of the area is highly vulnerable to land degradation and desertification, which could in turn harm other areas in thenear future. The satellite data used in this study enabled the researchers to quickly and accurately evaluate desertification, according to which75% compatibility was found between the ground truth (from 200 points) and estimations.

However,the low resolution of MODIS products was a significant limitation in the current study, leading to a mismatch between some parameters. Nonetheless, thefuture advancement of sensing technology can resolve this problem and further improve remote sensing application in desertification evaluation studies.

It appears that lack of vegetation due to climatic and edaphic measures along with anthropogenic factors such as overgrazing, improper agriculture, land conversion, and excessive withdrawal of groundwater resources are responsible for the Joghatay region's high vulnerability to desertification. As the region was found to be highly vulnerable to desertification, land managers need to adopt suitable managerial plans to prevent further aggravation of the situation and mitigate its consequences.

References

1. Abdollahi A., Nezhad M.P. and Pradhan B., 2019a. Determining the desertification risks of the Mashhad regions using integrated indices based on the AHP method, 2019 13th International Conference on Sensing Technology (ICST), pp. 1-6.
2. Abdollahi A., Nezhad M.P. and Pradhan B., 2019b. Investigation of the Vegetation Cover and the Vulnerability of the Mashhad Regions to Desertification by Using MODIS Image and EVI, 2019 IEEE International Conference on Cybernetics and Computational Intelligence (CyberneticsCom), pp. 46-49.
3. Akbari M., Memarian H., Neamatollahi E., Jafari Shalamzari M., Alizadeh Noughani M. and Zakeri D. 2021. Prioritizing policies and strategies for desertification risk management using MCDM–DPSIR approach in northeastern Iran. Environment, Development and Sustainability Vol 23: 2503-2523.

4. Akbari M., Shalamzari M.J., Memarian H. and Gholami A. 2020. Monitoring desertification processes using ecological indicators and providing management programs in arid regions of Iran. Ecological indicators Vol 111: 106011.
5. Chen H., Zhang W. and Jafari Shalamzari M. 2019. Remote detection of human-induced evapotranspiration in a regional system experiencing increased anthropogenic demands and extreme climatic variability. International Journal of Remote Sensing Vol 40: 1887-1908.
6. Daliakopoulos I., Tsanis I., Koutroulis A., Kourgialas N., Varouchakis A., Karatzas G. and Ritsema C. 2016. The threat of soil salinity: A European scale review. Sci Total Environ Vol 573: 727-739. https://doi.org/10.1016/j.scitotenv.2016.08.177
7. Darkoh M.B.K. 1998. The nature, causes and consequences of desertification in the drylands of Africa. Land Degradation & Development Vol 9: 1-20.
8. Dharumarajan S., Bishop T.F., Hegde R. and Singh S.K. 2018. Desertification vulnerability index—an effective approach to assess desertification processes: A case study in Anantapur District, Andhra Pradesh, India. Land Degradation & Development Vol 29: 150-161.
9. Didan K., Munoz A.B., Solano R. and Huete A. 2015. MODIS vegetation index user's guide (MOD13 series). University of Arizona: Vegetation Index and Phenology Lab
10. Du L., Tian Q., Yu T., Meng Q., Jancso T., Udvardy P. and Huang Y. 2013. A comprehensive drought monitoring method integrating MODIS and TRMM data. Int J Appl Earth Obs Geoinf Vol 23: 245-253. https://doi.org/10.1016/j.jag.2012.09.010
11. Fathi A., Jafari R. and Soltani S. 2015. Performance comparison of MEDALUD, MICD and FAO-UNEP desertification mapping models in the desertification hotspot of Jarghoyeh region, Isfahan province. Journal of Science and Technology of Agriculture and Natural Resources Vol 19: 299-310.
12. Ferreira T.R., Pace F.T.D., Silva B.B.D. and Delgado J.R. 2017. Identification of desertification-sensitive areas in the Brazilian Northeast through vegetation indices. Engenharia Agrícola Vol 37: 1190-1202.
13. Gajos M. and Sierka E. 2012. GIS Technology in Environmental Protection: Research Directions Based on Literature Review. Polish Journal of Environmental Studies Vol 21: 241-248.
14. Görener A. 2012. Comparing AHP and ANP: an application of strategic decisions making in a manufacturing company. International Journal of Business and Social Science Vol 3: 194-208.
15. Jafari Shalamzari M., Zhang W., Gholami A. and Zhang Z. 2019. Runoff Harvesting Site Suitability Analysis for Wildlife in Sub-Desert Regions. Water Vol 11: 1944.
16. Jain A., Nandakumar K. and Ross A. 2005. Score normalization in multimodal biometric systems. Pattern recognition Vol 38: 2270-2285.
17. Kaviani N., Onagh M., Sadodin A. and Filekesh E. 2014. Comparing efficiency of Iranian desert hazard assessment models, namely MICD and IMDPA (Case study: Sabzevar region). Journal of Water and Soil Conservation Vol 21: 1-28.
18. Kogan F.N. 1995. Application of vegetation index and brightness temperature for drought detection. Adv Space Res Vol 15: 91-100. https://doi.org/10.1016/0273-1177(95)00079-T
19. Kosmas C., Kirkby M.J. and Geeson N., 1999. Medalus Project: Mediterranean Desertification and Land Use. Manual on KEY INDICATORS of Desertification and Mapping Environmentally Sensitive Areas. Publication of European Union, Brussels,

Beligium.
20. Mehta M., Saha S. and Agrawal S. 2013. Evaluation of Indices and Parameters Obtained from Optical and Thermal Bands of Landsat 7 ETM+ for Mapping of Salt-Affected Soils and Water-Logged Areas. Asian Journal of Geoinformatics Vol 12:
21. Oldeman L., Hakkeling R., Sombroek W. and Batjes N., 1991. Global assessment of human-induced soil degradation (GLASOD), World map of the status of human-induced soil degradation. Wageningen, Netherlands: Winand Staring Centre–ISSSFAO–ITC.
22. Orimoloye I.R., Belle J.A. and Ololade O.O. 2021. Drought disaster monitoring using MODIS derived index for drought years: A space-based information for ecosystems and environmental conservation. Journal of Environmental Management Vol 284: 112028.
23. Parvari S.H., Pahlavanravi A., Moghaddam Nia A.R., Dehvari A. and Parvari D. 2011. Application of methodology for mapping environmentally sensitive areas (ESAs) to desertification in dry bed of Hamoun Wetland (Iran). ECOPERSIA 65-80.
24. Pashaei M., Rashki A. and Sepehr A. 2017. An integrated desertification vulnerability index for Khorasan-Razavi, Iran. Natural Resources and Conservation Vol 5: 44-55.
25. Saaty T.L. 2008. Decision making with the analytic hierarchy process. International journal of services sciences Vol 1: 83-98.
26. Sepehr A. and Parvian N. 2012. Desertification vulnerability mapping and prioritize confronting strategies in Khorasan Razavi province based on the nartbh pramsh algorithm. Earth Sci. Res. J Vol 8: 58-71.
27. Sepehr A., Zucca C. and Nowjavan M.R. 2014. Desertification Inherent Status Using Factors Representing Ecological Resilience. British Journal of Environment and Climate Change Vol 4: 279.
28. Shihab T.H. and Al-hameedawi A.N. 2020. Desertification Hazard Zonation in Central Iraq Using Multi-criteria Evaluation and GIS. Journal of the Indian Society of Remote Sensing Vol 48: 397-409.
29. Shiravi M. and Sepehr A. 2017. Fuzzy Based Detection of Desertification-Prone Areas: A Case Study in Khorasan-Razavi Province, Iran. Natural Resources and Conservation Vol 5: 1-12.
30. ten Have H. and Neves M.d.C.P., 2021. Rio Declaration on Environment and Development, Dictionary of Global Bioethics. Springer, pp. 51-51.
31. Tollefson J. and Gilbert N. 2012. Earth summit: Rio report card. Nature News Vol 486: 20.
32. Velasquez M. and Hester P.T. 2013. An analysis of multi-criteria decision making methods. International journal of operations research Vol 10: 56-66.
33. Vogt J., Safriel U., Von Maltitz G., Sokona Y., Zougmore R., Bastin G. and Hill J. 2011. Monitoring and assessment of land degradation and desertification: towards new conceptual and integrated approaches. Land Degradation & Development Vol 22: 150-165.
34. Wang L., Seki K., Miyazaki T. and Ishihama Y. 2009. The causes of soil alkalinization in the Songnen Plain of Northeast China. Paddy and Water Environment Vol 7: 259-270. https://doi.org/10.1007/s10333-009-0166-x